HUPD-9208
TU-404
KEK-TH-333
KEK preprint 92-39
May 1992

Evaluating Cross Sections at TeV Energy Scale by HELAS *

I. WATANABE[1], H. MURAYAMA[2] and K. HAGIWARA[3]

[1] *Department of Physics, Hiroshima University, Higashi-Hiroshima 724, Japan*

[2] *Department of Physics, Tohoku University, Sendai 980, Japan*

[3] *Theory Group, KEK, Tsukuba, Ibaraki 305, Japan*

ABSTRACT

A Fortran subroutine package HELAS (HELicity Amplitude Subroutines) is briefly reported. Helicity amplitudes of arbitrary tree–level Feynman diagrams in an arbitrary renormalizable theory can be evaluated easily by HELAS. The HELAS subroutines treat carefully the gauge theory cancellations and the collinear singularities, so as not to lose numerical accuracies of the amplitudes at the TeV energy scale.

* Invited talk presented by I. Watanabe at *"The Third Workshop on Japan Linear Collider"*, KEK, Feb. 25-27, 1992

§1. How to calculate cross sections

As is well known, cross sections can be obtained by squaring the amplitude, summing/averaging it over the final/initial state spins, integrating over the phase space, and dividing it by the flux factor:

$$\sigma \ = \ \frac{1}{\text{Flux}} \int d\Phi \overline{\sum_{\text{spin}}} |\mathcal{M}|^2 \quad . \tag{1}$$

However, to calculate the matrix element $\mathcal{M}$ and to find a good parameterization of the phase space Φ are *not always* easy jobs, even in tree–level computations.

The difficulties in getting $\mathcal{M}$ come from the following points. Processes of our interest at TeV energies typically have

(a) many Feynman diagrams

and

(b) many final state particles.

Then a tough work is necessary to evaluate all the necessary diagrams. In order to manage many diagrams and many particles, we have to *computorize* at least some parts of the calculations. Furthermore, we encounter subtle

(c) gauge theory cancellation

in electroweak processes at high energies, which cause severe numerical problems.

The HELAS[1] system is designed to overcome the above difficulties. We list below the keynotes of HELAS.

- HELAS is a set of FORTRAN77 Subroutines for numerical evaluations of HELicity Amplitudes.
- HELAS can be used to evaluate any tree–level Feynman diagrams in an arbitrary renormalizable theory.
- HELAS gives amplitudes accurately at and below the TeV energy scale with single precision computations.
- HELAS allows us to evaluate a diagram by a simple sequence of CALL SUBROUTINE statements.
- HELAS can be used to make a highly efficient program to evaluate multi-particle amplitudes.
- HELAS is compact and portable.

Unlike some more challenging projects which aim at a full–automatic computation of cross sections,[2–5] HELAS supports only a part of the whole job, i.e. to evaluate helicity amplitudes. It does the job, however, with a full generality and at a very high level of numerical efficiency and accuracy. HELAS is only a set of *subroutines*, with the help of which you write a *main routine* to evaluate Feynman diagrams; this, however, is very easy since an arbitrarily complicated Feynman diagram can be programmed by a simple sequence of CALL HELAS-SUBROUTINE statements. The efficiency of the main programs with HELAS subroutines grows more and more as the number of Feynman diagrams proliferates. The final task of summing over helicities and the phase space should be made by a standard numerical integration package, such as BASES[6] or VEGAS.[7] It is of course possible that the HELAS subroutines can be used as a part of a more automatic system for evaluating cross sections, to improve the numerical efficiency of the existing systems by more than an order of magnitude.

§2 . How to calculate amplitudes by HELAS

Here we show you how to evaluate $\mathcal{M}$ by HELAS by an example. You'll find more details of HELAS in Ref. [1].

Let us first remind you of the general characteristics of tree–level diagrams. As you see from the word 'tree', they have a common structure. There may be many external lines. As they approach the center of a Feynman diagram, the external lines meet to give an off-shell internal line, and then meet again to make another internal line, until all the lines meet at a single point. The basic idea of HELAS is to begin with the external lines by creating the wavefunctions explicitly in a fixed notation, and to give rules to join the lines. Any amplitudes can be computed as follows; first, the external wave functions are evaluated as functions of the particle momenta and helicities. Second, off-shell scalar/spinor/vector (S/F/V) lines obtained from the external lines via renormalizable vertices are evaluated as functions of the external wave functions. This second step can be repeated, giving internal off-shell lines as functions of external off-shell lines, until all the off-shell lines meet.

2.1 Example: $e^-e^+ \to W^-W^+$

Let us choose as an example the t-channel neutrino exchanging diagram of the process $e^-e^+ \to W^-W^+$ (Fig. 1). It has four external lines; electron ($|\, e^- >$) and positron ($< e^+ \,|$) spinors, and W^-, W^+ vector bosons. These external wavefunctions can be obtained by calling wave function subroutines by specifying the four-momenta and helicities of these particles (Fig. 1(a)). Once the external wavefunctions are obtained this way, you can compute an off-shell neutrino wavefunction $|\, \nu_e, W^-, e^- >$ from the external wavefunctions W^- and $|\, e^- >$ with the appropriate weak coupling at the ν_e-W^-–e^- vertex (Fig. 1(b)). Finally by joining this off-shell neutrino wavefunction $|\, \nu_e, W^-, e^- >$ and the remaining external lines $< e^+ \,|$ and

W^+, you obtain the contribution of the diagram (Fig. 1(c)) to the helicity amplitude, $\mathcal{M}=< e^+ \mid W^+ \mid \nu_e, W^-, e^- >$, which is just a complex number.

The above procedures can be performed by the following FORTRAN codes.

(a) external wavefunctions:
```
    CALL IXXXXX(PEM,EMASS,NHEM,+1 , EM)             |e- >
    CALL OXXXXX(PEP,EMASS,NHEP,-1 , EP)             < e+ |
    CALL VXXXXX(PWM,WMASS,NHWM,+1 , WM)             W-_mu
    CALL VXXXXX(PWP,WMASS,NHWP,+1 , WP)             W+_nu
```
(b) off-shell wavefunction:
```
    CALL FVIXXX(EM,WM,GWF,NMASS,NWIDTH , FVI)       | nu_e, W-, e- >
```
(c) amplitude:
```
    CALL IOVXXX(FVI,EP,WP,GWF , AMP)        < e+ | W+ | nu_e, W-, e- >
```

You can see here how simple the HELAS grammar is. First, the subroutine IXXXXX computes an external flowing-In fermion wavefunction, OXXXXX an external flowing-Out fermion wavefunction, and VXXXXX gives an external Vector wavefunction. Second, the vertex subroutine FVIXXX combines an flowing-In fermion and a Vector boson to give an off-shell Fermion wavefunction FVI. Finally, the subroutine IOVXXX joins flowing-In and flowing-Out fermions with a Vector boson to give an amplitude. As you see here, all HELAS subroutines are named systematically. You can easily remember the role of a HELAS subroutine from its naming.

We will explain the inputs and the outputs of the above subroutines briefly. The external wavefunction subroutines (a) have four inputs and one output. The inputs are the particle four-momentum, mass, helicity, and an index which distinguishes between a particle and an anti-particle for a fermion, or if the particle is in the final state or in the initial state in case of a boson. Here the four-momentum is given as a real four-dimensional array (0:3). The output of these subroutines is a six-dimensional array (6) of complex values, the first four entries give the wavefunction and the latter two complex numbers give the particle four-momentum.

The input variables of the off-shell line subroutine (b) are the wavefunctions EM and WM obtained above, the coupling constant GWF, the mass NMASS and the width NWIDTH of the output particle. The coupling constant GWF of fermion–fermion–vector vertices are real two-dimensional arrays, one for each fermion chirality. The output FVI is the off-shell neutrino wavefunction, which is again a six-dimensional array of complex values.

The amplitude subroutine (c) has several wavefunctions (FVI,EP,WP) and a coupling constant (GWF) as inputs, and just one output (AMP), which is a complex variable.

There is actually another way to obtain the same amplitude by HELAS in the above example. The off-shell neutrino wavefunction can be obtained from the external positron and W^+ boson, $< e^+, W^+, \nu_e \mid$, rather than from the external electron and W^-, $\mid \nu_e, W^-, e^- >$, as in the previous case. The same amplitude is now evaluated as $< e^+, W^+, \nu_e \mid W^- \mid e^- >$. The FORTRAN program in this case is as follows.

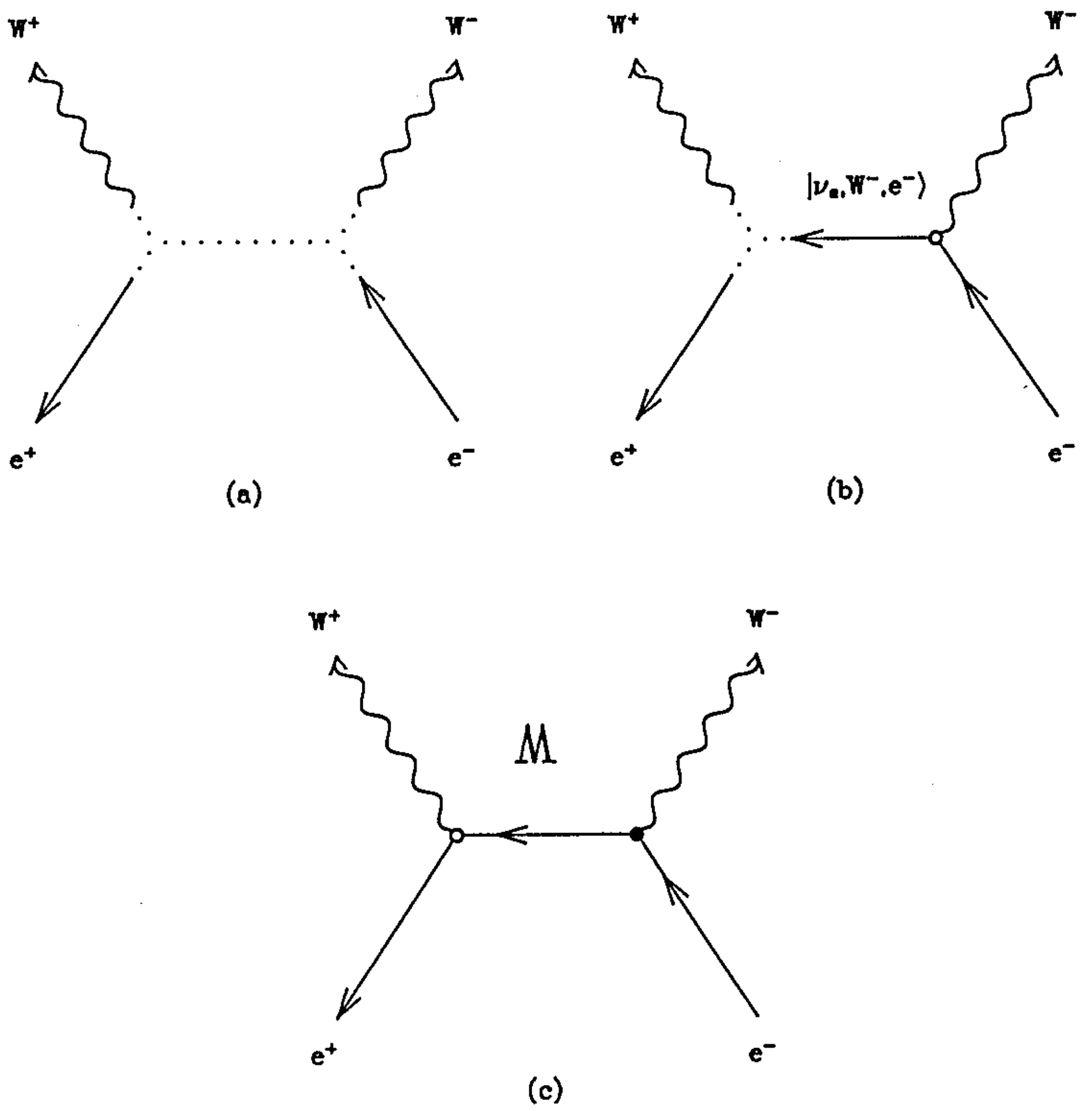

Figure 1: Illustration of how we evaluate the t-channel neutrino exchange amplitude of the process $e^-e^+ \to W^-W^+$ with HELAS. (a) Preparing the external wavefunctions. (b) Joining the wavefunctions to get an off-shell neutrino wavefunction via the ν_e–W^-–e^- vertex. (c) Obtaining the amplitude by joining the off-shell wavefunction with the remaining external lines at the e^+–W^+–ν_e vertex.

(a′) external wavefunctions: same as (a)

(b′) off-shell wavefunction:

```
    CALL FVOXXX(EP,WP,GWF,NMASS,NWIDTH , FVO)
```
$< e^+, W^+, \nu_e \,|$

(c′) amplitude:

```
    CALL IOVXXX(EM,FVO,WM,GWF , AMP)
```
$< e^+, W^+, \nu_e \,|\, W^- \,|\, e^- >$

In general, the number of ways to write down a FORTRAN program for a tree diagram by HELAS is just the number of the vertices of the diagram. You can utilize this freedom for checking the numerical accuracy of the results or finding bugs in the program.

When using HELAS, it is quite easy to incorporate decays of final state particles without losing the spin correlations. For instance, if you want an amplitude of the above process with a subsequent decay of $W^- \to \bar{u}d$, all you should do is to replace the "CALL VXXXXX(PWM,... , WM)" line in the above example by the following three FORTRAN lines:

(a″) external wavefunctions:

```
    CALL IXXXXX(PU ,UMASS,NHU ,-1 , FU)
    CALL OXXXXX(PD ,DMASS,NHD ,+1 , FD)
```
$|\, \bar{u} >$ and $< d \,|$ respectively

(b″) off-shell wavefunction of W^-:

```
    CALL JIOXXX(FU,FD,GWF,WMASS,WWIDTH , WM)
```
$J^\mu_{W^-}(< d \,|, |\, \bar{u} >)$

Here JIOXXX is a subroutine which computes an off-shell vector current (J) from the flowing-In and -Out fermions. The final output AMP is now the amplitude for the process $e^+e^- \to \bar{u}dW^+$ via the same diagram.

2.2 HELAS subroutines

In this subsection we explain what kinds of subroutines are available in the HELAS package. As you have already seen in the previous subsection, HELAS has several subroutines which compute external wavefunctions, some others compute off-shell wavefunctions, and also some subroutines which compute the amplitudes of diagrams at certain vertices. For example, there are five HELAS subroutines for the fermion–fermion–vector vertex; FVIXXX, FVOXXX, JIOXXX, IOVXXX have already appeared in the above examples, and one more special subroutine J3XXXX which computes a specific combination of the Z boson and the photon currents. You might think that there are too many possibilities to find a complete set of joining rules, but in fact they can all be classified into a finite set in renormalizable theories. We show all the possible joints of renormalizable theories in Table 1.

The whole HELAS package can be divided into three types of subroutines;

- External line subroutines
- Vertex subroutines
- Utility subroutines

The external lines are computed by the four subroutines IXXXXX, OXXXXX, VXXXXX and SXXXXX, for which the particle four-momentum and helicities should be given as inputs (Table 2).

Table 1: List of the possible vertices in renormalizable theories. All these vertices are incorporated in the HELAS system.

Vertex	interaction
FFV	vector or axial vector couplings
FFS	Yukawa couplings
VVV	Yang-Mills couplings
VVS	Higgs interaction
SSV	scalar gauge couplings
SSS	scalar self-couplings
VVVV	Yang-Mills couplings
VVSS	scalar gauge couplings (seagull)
SSSS	scalar self-couplings

At each type of a vertex, we can obtain either one off-shell internal line, or an amplitude (Table 3). You may worry that there are too many subroutines to remember. However, the names of the subroutines and their inputs/outputs are systematically determined, and one can easily guess the name of the desired subroutine, or find out its function from its name. The codes `I,O,V,S` mean the *input* flowing-`In` fermion, flowing-`Out` fermion, `V`ector boson, `S`calar boson, respectively, and the codes `F,J,H` refer to the *output* `F`ermion, vector, scalar wavefunctions, respectively.

There are also some utility subroutines (Table 4). Most of them may be used for setting up phase space variables. They can compute four-momenta from angles, and can also rotate or boost four-momenta. The rest of the utility subroutines prepare default coupling constant values for the Standard Model. The outputs of these subroutines should be regarded as templates for defining the couplings appropriate for the HELAS subroutines. These subroutines provide all possible coupling constants in the Standard Model except for the Kobayashi–Maskawa matrix elements, which should be multiplied to the amplitudes 'by hand' outside the subroutines.

§3. How to calculate amplitudes accurately

It is a non-trivial task to obtain accurate results when you compute amplitudes numerically. The numerals used in HELAS are single precisions, i.e. `INTEGER*2`, `REAL*4` and `COMPLEX*8`. The output amplitudes or wavefunctions are also given in the single precision complex number `COMPLEX*8` (or its array). Though the choice of the single precision makes the program fast, one may wonder whether it is numerically accurate enough. We will critically examine the numerical accuracies below for processes with very bad gauge theory cancelations. It is shown that the choice of single precision is always enough for the processes below several TeV at the 1% level, usually up to $\sim$ 100 TeV. The HELAS subroutines have been coded with a great care, in order that they do not lose numerical accuracy, while being efficient, within their expected functions. Furthermore, the electroweak gauge theory cancellations and the photon/electron collinear singularities have been cautiously treated in HELAS.

Table 2: List of 'External Lines' Subroutines.

External line	Subroutine
Flowing-In Fermion	IXXXXX
Flowing-Out Fermion	OXXXXX
Vector Boson	VXXXXX
Scalar Boson	SXXXXX

Table 3: List of the vertex subroutines in **HELAS** system.

Vertex	Inputs	Output	Subroutine
FFV	FFV	Amplitude	IOVXXX
	FF	V	JIOXXX, J3XXXX
	FV	F	FVIXXX, FVOXXX
FFS	FFS	Amplitude	IOSXXX
	FF	S	HIOXXX
	FS	F	FSIXXX, FSOXXX
VVV	VVV	Amplitude	VVVXXX
	VV	V	JVVXXX
VVS	VVS	Amplitude	VVSXXX
	VS	V	JVSXXX
	VV	S	HVVXXX
VSS	VSS	Amplitude	VSSXXX
	SS	V	JSSXXX
	VS	S	HVSXXX
SSS	SSS	Amplitude	SSSXXX
	SS	S	HSSXXX
VVVV	VVVV	Amplitude	WWWWXX, W3W3XX
	VVV	V	JWWWXX, JW3WXX
VVSS	VVSS	Amplitude	VVSSXX
	VSS	V	JVSSXX
	VVS	S	HVVSXX
SSSS	SSSS	Amplitude	SSSSXX
	SSS	S	HSSSXX

Table 4: List of 'Utility' Subroutines.

Utilities for Momentum Manipulations:

p^μ(energy,mass,costh,phi)	: set up momentum	MOMNTX
p_1^μ & p_2^μ	: set up two momenta in c.m. frame	MOM2CX
p_{boosted}	: Lorentz boost of momentum	BOOSTX
p_{rotated}	: rotation of momentum	ROTXXX

Standard Model Coupling Constants:

for VVV,VVVV vertices	COUP1X
for FFV vertices	COUP2X
for VVS,SSS,VVSS,SSSS vertices	COUP3X
for FFS vertices	COUP3X

3.1 Gauge Theory Cancellations

Special cares on the gauge theory cancellation are paid in the subroutines J3XXXX, VVVXXX, WWWWXX, JWWWXX, W3W3XX and JW3WXX.

The subroutine J3XXXX computes the weighted sum W^3,

$$W_\mu^3 = A_\mu \sin\theta_W + Z_\mu \cos\theta_W \ , \tag{2}$$

of the photon and Z currents emerging from the same fermion lines. Whenever you have Z- and photon-exchange lines between a common fermion line and a W self-interaction vertex, then it is always better to use J3XXXX. The cancellation between the Z- and photon-exchange contribution is arranged analytically in J3XXXX whenever possible, which makes J3XXXX numerically more reliable than computing the Z- and photon-exchange amplitudes separately and adding them afterwards.

The subroutine VVVXXX computes the Feynman amplitudes from three vector bosons. What we compute here is the following T-matrix element:

$$\begin{aligned}\texttt{VERTEX} \ &= \ -\texttt{G}\{((p^- - p^+)\cdot V^3)(V^-\cdot V^+) + ((p^+ - p^3)\cdot V^-)(V^+\cdot V^3) \\ &\quad +((p^3 - p^-)\cdot V^+)(V^3\cdot V^-)\}\ ,\end{aligned} \tag{3}$$

where $V^\pm, V^3$ are vector boson wavefunctions, and $p^\pm, p^3$ are their momenta, G is the coupling constant. However, there is a gauge theory cancellation between the three terms, which can jeopardize single-precision manipulations, when all three currents have large longitudinal or scalar components. Fortunately, there is an expression which can be used to avoid the worst cancellation at high energies:

$$\begin{aligned}\texttt{VERTEX} \ = \ -\texttt{G} \ &\{((p^- - \alpha_- V^- - p^+ + \alpha_+ V^+)\cdot V^3)(V^-\cdot V^+) \\ &+((p^+ - \alpha_+ V^+ - p^3 + \alpha_3 V^3)\cdot V^-)(V^+\cdot V^3) \\ &+((p^3 - \alpha_3 V^3 - p^- + \alpha_- V^-)\cdot V^+)(V^3\cdot V^-)\}\ ,\end{aligned} \tag{4}$$

which is identical to eq. (3) for any set of complex numbers α_-, α_+, α_3. With our choice of α's;

$$\begin{aligned}\alpha_- &= p_0^-/V_0^- \ , \\ \alpha_+ &= p_0^+/V_0^+ \ , \\ \alpha_3 &= p_0^3/V_0^3 \ ,\end{aligned} \tag{5}$$

we can significantly reduce the numerical values of the scalar and longitudinal component of the vector currents.

The problem associated with gauge theory cancellations repeats again at the $VVVV$ type interactions. In any processes with a four-vector-boson vertex, there also appear two of the t-, s- or u-channel vector boson exchange diagrams as well. There is a subtle gauge theory cancellation between these diagrams. Even worse than in the case of the VVV vertex, we should expect a further cancellation with the Higgs boson exchange diagram when its mass is small compared to the energy.

To improve numerical accuracy of the program in the presence of such a cancellation, we combine all the $VVVV$ diagrams into a single subroutine, which is computed at the double precision level internally. By combining the three diagrams into a single subroutine, the HELAS program is made more compact. For example, two-photon production of a W-pair can be computed with a single amplitude subroutine, W3W3XX.

```
CALL VXXXXX(PWM,WMASS,NHWM,+1 , WM)
CALL VXXXXX(PWP,WMASS,NHWP,+1 , WP)
CALL VXXXXX(PA1,0.    ,NHA1,-1 , A1)
CALL VXXXXX(PA2,0.    ,NHA2,-1 , A2)
CALL W3W3XX(WM,A1,WP,A2,GWWA,GWWA,WMASS,WWIDTH , AMP)
```

That's all. Here **W3W3XX** computes the four-point scattering amplitude, including the contact, as well as t- and u-channel W exchange contributions. The same strategy has been adopted in the JW3WXX subroutine to evaluate $W/Z/\gamma$ currents from the four-W vertex. Four charged W boson vertices are calculated by **WWWWXX** and JWWWXX subroutines. There also, the photon exchanging diagrams and the Z exchanging diagrams are included together with the contact four-W boson diagram.

3.2 Collinear Singularities

At high energies we also encounter collinear photon and/or electron singularities. Since the worst singularities appear at the electron–photon vertices with an electron initial state, it is useful to have a numerically safe expression for the collinear photon or electron emerging from the initial electron beam. We provide special subroutines EAIXXX, EAOXXX and JEEXXX for the particular γ–e–e vertex for this purpose. Even though the quantitative predictions for such a configuration require careful treatment of the QED radiative effects (multiple soft photon emissions), we find it very useful to be able to compute accurately exact tree–level amplitudes at all kinematical configurations. These three special subroutines assume that the initial e^- and e^+ momenta are along the z-axis, and we use $\sin\frac{\theta}{2}$ *and* $\cos\frac{\theta}{2}$ of the final $e^\pm$ or γ scattering angle as inputs, which are found to be useful in efficiently evaluating the electron/photon propagator, as well as the relevant products of the external wavefunctions, to the necessary accuracy. In the JEEXXX subroutine the output γ current is modified to avoid a subtle gauge theory cancellation by shifting it by a term proportional to its four-momentum q^μ,

$$J_A^\mu(< e'\,|\,,\;|\,e >) \rightarrow J_A^\mu - \frac{J^0}{q^0} q^\mu \quad . \tag{6}$$

The proof that we can make the above shift of the γ current both in the initial e^- and e^+ cannels simultaneously (the so-called quasi-two-photon processes) is given in Ref. [1], which is non-trivial in the electroweak theory where the photon is partly a non-Abelian gauge boson.

These three special subroutines are found numerically very efficient that they can deal with the collinear singularities practically at arbitrary high energies. The only limitation of the present HELAS system in the collinear configuration is met only when two or more photons or $e^{\pm}$ are emitted along the initial $e^{\pm}$ beam direction. It is our belief that such configurations should be treated by a more specialized program for initial state radiations.

3. 3 Error Estimations

The numerical accuracy of the HELAS outputs have been tested carefully in the processes $e_L^- e_R^+ \to W_L^- W_L^+$ and $W_L^- W_L^+ \to W_L^- W_L^+$, which essentially set the limitation of the use of HELAS at super high energies. Here $W_L^{\pm}$ denote longitudinally polarized $W^{\pm}$ bosons.

There are two diagrams in the former process, i.e. the t-channel ν_e exchange and the s-channel W^3 exchange diagrams. It is well known that the amplitude of each diagram is proportional to $(E/m_W)^2$ in the high energy limit, where E is the beam energy. However, the sum of the two amplitudes behaves as a constant asymptotically, due to a gauge theory cancellation between two sets of diagrams. There is hence a cancellation of order $(E/m_W)^2$ terms which is about 10^2 at $\sqrt{s}$ = 1 TeV, and 10^4 at $\sqrt{s} = 10$ TeV. Since HELAS computes amplitudes diagram by diagram, it is impossible to be efficient in the gauge theory cancellation between diagrams of different structure. There is a possibility that the HELAS output may not reproduce the required cancellation in the above process.

We first study the numerical accuracy of the HELAS output by comparing it with the analytic formula for the process $e_L^- + e_R^+ \to W_L^- + W_L^+$ (Fig. 2). The solid lines are the magnitudes of s-channel amplitude $\mathcal{M}_s$ (a), t-channel amplitude $\mathcal{M}_t$ (b) and the sum $\mathcal{M} = \mathcal{M}_s + \mathcal{M}_t$ (c), as functions of the c.m. scattering angle $\cos\theta$ at three energies $\sqrt{s} = 0.2$, 1, and 10 TeV. The dots represent the *relative* errors of the numerical results at each $\cos\theta$ point. The orders of the errors in the amplitudes as compared with the above analytic formulae averaged over many $\cos\theta$ points are summarized in Table 5. You can see from Fig. 2 and Table 5 that the HELAS amplitude is accurate at the level of 10^{-4} up to a few TeV against the gauge theory cancellation in this process.

The severest gauge theory cancellation in the $2 \to 2$ process is expected to take place in the longitudinally polarized weak boson scattering processes $W_L^- W_L^+ \to W_L^- W_L^+$, $Z_L Z_L$ at high energies when the Higgs boson is light. If the off-shell weak boson is in the unitary gauge, the helicity amplitude of the above processes receives two types of contributions: $\mathcal{M}_W$ is the sum of all the weak boson exchange amplitudes, and $\mathcal{M}_H$ is the sum of the s- and t-channel Higgs boson exchange amplitudes. In the high energy limit $E \gg m_W$, both the amplitudes $\mathcal{M}_W$ and $\mathcal{M}_H$ are known to behave as $(E/m_W)^2$ while their sum remains as a constant at $E \gg m_H$. What make the problem worse in this process is that, each diagram contributing to $\mathcal{M}_W$ behaves as $(E/m_W)^4$ initially, and it is only because of the electroweak gauge invariance of all the couplings appearing in these diagrams that the sum $\mathcal{M}_W$ behaves as $(E/m_W)^2$. Therefore, we should expect cancellation among order $(E/m_W)^4$ terms in these processes, leaving only the final amplitude of $\sim$1. Note

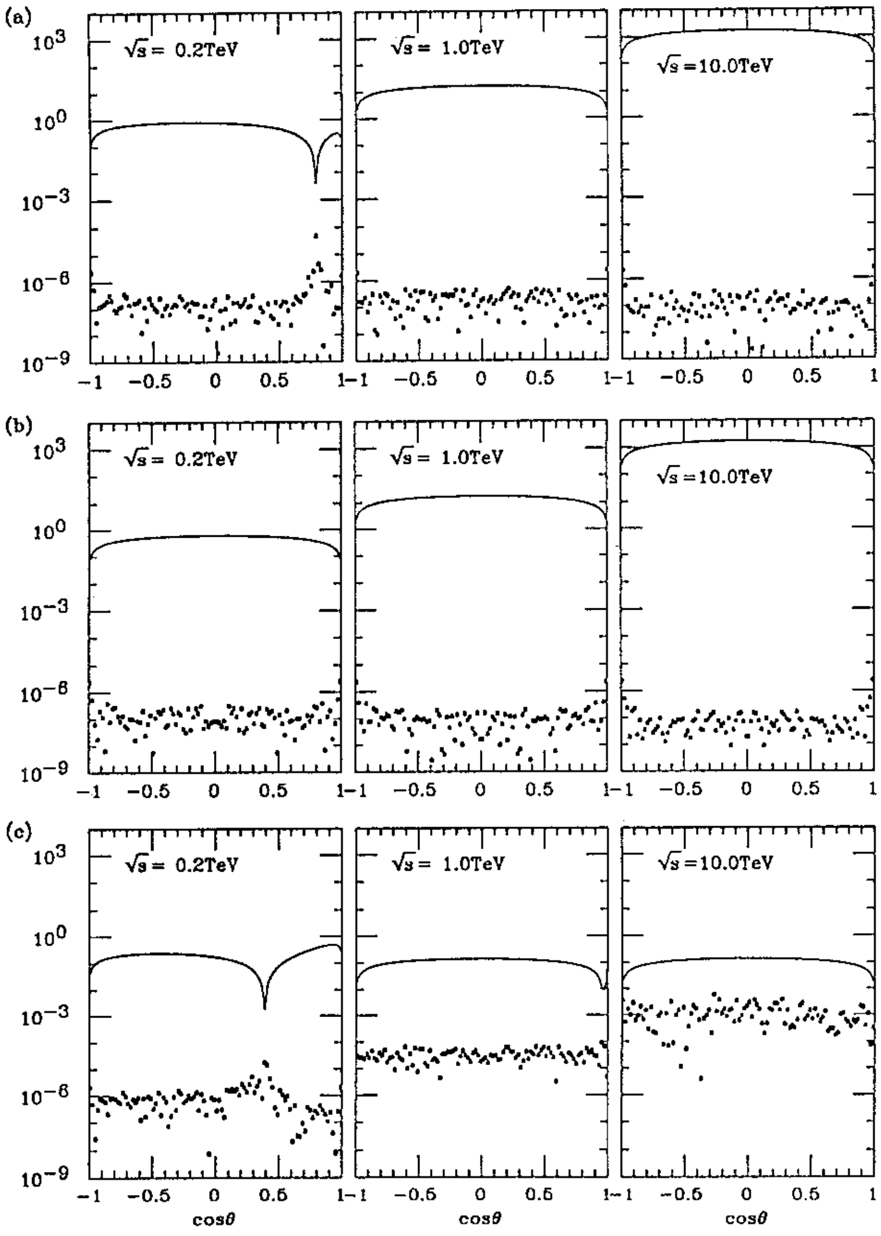

Figure 2: The test of the numerical accuracies in the process $e_L^- e_R^+ \to W_L^- W_L^+$. The figures (a) show the s-channel γ and Z exchange amplitude, (b) the t-channel ν_e exchange amplitude, and (c) their sum. The solid lines are the amplitudes plotted vs. $\cos\theta$ in the c.m. frame, computed by the analytic expressions. The dots represent the *relative* error of the HELAS amplitudes.

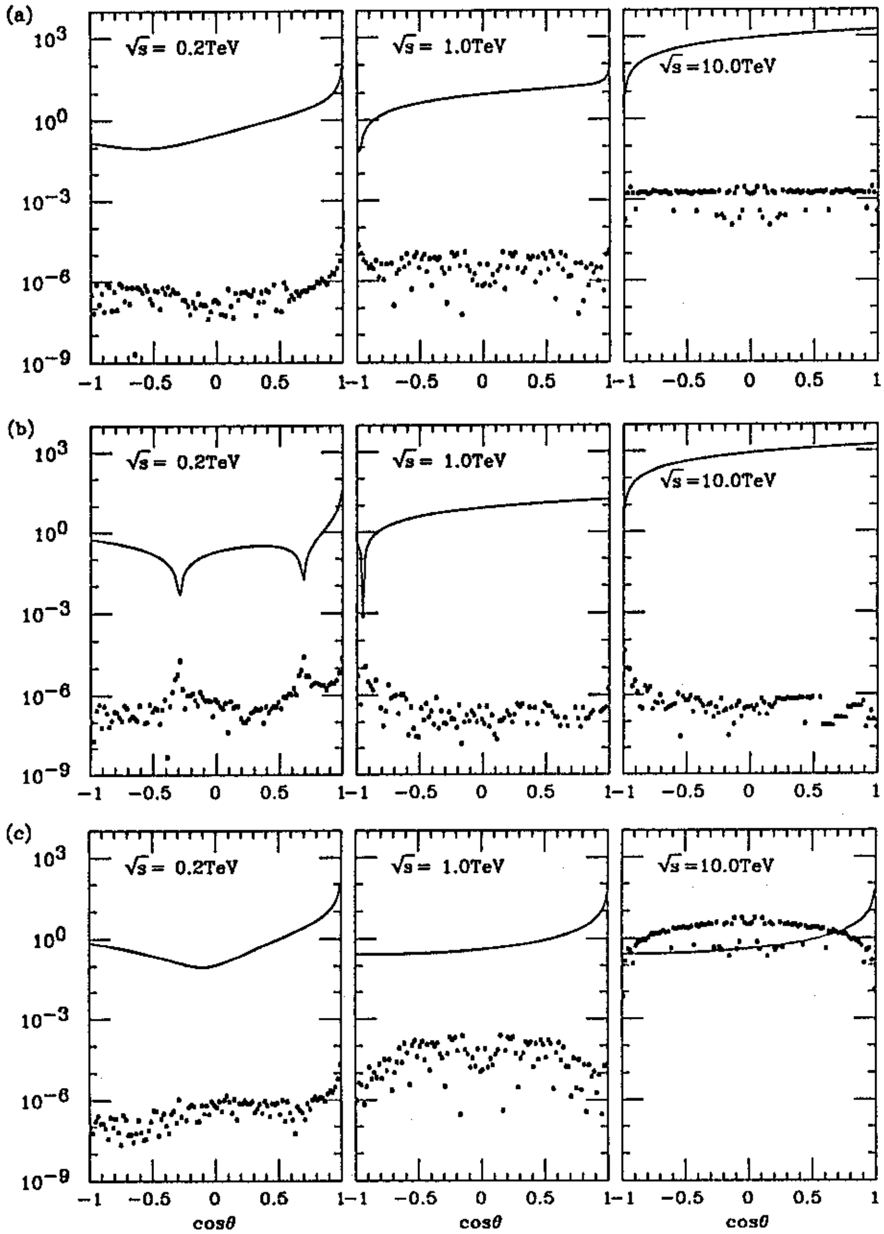

Figure 3: The test of the numerical accuracies in the process $W_L^- W_L^+ \to W_L^- W_L^+$. The figures (a) show the sum of s and t-channel γ, Z exchange amplitudes as well as the four-point contact diagram, (b) the s- and t-channel Higgs boson exchange amplitude, and (c) their sum. The solid lines are the amplitudes plotted vs. $\cos\theta$ in the c.m. frame, computed by DHELAS. The dots represent the *relative* error of the HELAS amplitudes.

Table 5: Average of the order of error for the amplitudes $\mathcal{M}_t$, $\mathcal{M}_s$ and $\mathcal{M}$ computed by HELAS. We set $\sin^2\theta_W$=0.23, m_W=80.0GeV, $m_Z=m_W/\cos\theta_W$, Γ_Z=0., and m_e=0.

$\sqrt{s}$	$\mathcal{M}_t$	$\mathcal{M}_s$	$\mathcal{M}$
0.2 TeV	$10^{-6.9}$	$10^{-7.0}$	$10^{-6.3}$
1.0 TeV	$10^{-6.8}$	$10^{-7.1}$	$10^{-4.5}$
10.0 TeV	$10^{-7.1}$	$10^{-7.2}$	$10^{-3.1}$

Table 6: Average of the order of error in the amplitudes $\mathcal{M}_W, \mathcal{M}_H$ and $\mathcal{M}$ computed by HELAS. The adopted parameters are $\sin^2\theta_W$=0.23, m_W=80.0GeV, $m_Z=m_W/\cos\theta_W$, Γ_Z=0., and m_H=0.

$\sqrt{s}$	$\mathcal{M}_W$	$\mathcal{M}_H$	$\mathcal{M}$
0.2 TeV	$10^{-6.6}$	$10^{-6.3}$	$10^{-6.5}$
1.0 TeV	$10^{-5.6}$	$10^{-6.8}$	$10^{-4.6}$
10.0 TeV	$10^{-2.9}$	$10^{-6.4}$	$10^{+0.1}$

that this factor is about 10^4 at $\sqrt{s} = 1$ TeV, and 10^8 at $\sqrt{s} = 10$ TeV.

We show in Fig. 3, the magnitude of the amplitudes for the process $W_L^- W_L^+ \to W_L^- W_L^+$ as functions of the c.m. scattering angle; $|\mathcal{M}_W|$ in (a), $|\mathcal{M}_H|$ for $m_H = 0$ in (b), and $|\mathcal{M}| = |\mathcal{M}_W + \mathcal{M}_H|$ in (c), at three energies $\sqrt{s} = 0.2$, 1 and 10 TeV. The dots represent the *relative* errors of the amplitudes evaluated by standard HELAS and those obtained by its double precision version DHELAS at each $\cos\theta$ point. The averages of the order of the errors are again summarized in Table 6.

We can clearly see from Fig. 3(a) and Table 6 that the numerical error of the single precision program increases rapidly with rising energies E for $\mathcal{M}_W$, exhibiting the cancellation among order $(E/m_W)^4$ terms resulting in the $(E/m_W)^2$ behavior. The numerical error in the Higgs boson exchange diagrams in $\mathcal{M}_H$ remains small (see Fig. 3(b) and the middle column of Table 6) since there is no subtle cancellation between the s- and t-channel exchange diagrams. The terms of order $(E/m_W)^2$ in $\mathcal{M}_W$ and $\mathcal{M}_H$ then cancel again in the sum, and the numerical accuracy of the standard HELAS program is lost at $\sqrt{s} = 10$ TeV, as can be seen from the dotted lines in Fig. 3(c) and the last column in Table 6.

It is worth noting here that the loss of numerical accuracy discussed above is solely due to the subtle gauge theory cancellation among several Feynman diagrams and that it has nothing to do with our choice of the unitary gauge for the weak boson propagators. In fact, we find no improvement in the numerical accuracy of the amplitudes when we evaluate all the relevant sub-amplitudes in the t'Hooft–Feynman gauge. See Ref. [1] for more detail.

In conclusion, the standard HELAS subroutines give reliable numerical results (error $<$ 1 %) in the region $m_{VV} \lesssim 50$ TeV for processes with three weak boson vertices, and at $m_{VV} \lesssim 3$ TeV in processes with four weak boson vertices. We do not anticipate any other sources of severe numerical inaccuracy in the use of the HELAS subroutines, as long as one makes proper use of the special subroutines EAIXXX, EAOXXX and JEEXXX when dealing with collinear singularities.

As demonstrated above the double precision version of HELAS, called DHELAS, shows no hint of numerical inaccuracy up to $m_{VV} \sim 10$ TeV. We may ask its help as the last resort, if a necessity arises. However, unlike HELAS, DHELAS is not portable. It can be supported only by a system which allows a COMPLEX*32 manipulation.

§4. How to check your program

Once you write down a HELAS code of a process of your interest, what you'll do next is to check your program. The HELAS_CHECK subroutines (sect. 4.1) are prepared to help you find bugs in your program. The package HELAS_CHECK also help you make the BRS invariance tests of the amplitudes (sect. 4.2) for the processes with one or more external vector bosons.

4.1 HELAS_CHECK

All the HELAS subroutines are designed to run as fast as possible. For this purpose, the HELAS subroutines do not check the appropriateness of the inputs at all. There are cases that FORTRAN77 does not give you any error messages no matter how inconsistent your inputs are. In such cases, run-time error messages from HELAS_CHECK may be helpful in identifying the bugs in your program.

Its use is just the same as HELAS, except that you should *link* HELAS_CHECK instead of HELAS when you compile the program. Then HELAS_CHECK will test the consistency of all the inputs of the subroutines. In cases where FORTRAN77 gives error messages, additional information from the HELAS_CHECK messages will make your job of identifying the error easier. In particular, possible typographical errors can easily be detected by HELAS_CHECK.

There are two levels of the run-time messages from HELAS_CHECK:

(a) HELAS-ERROR

(b) HELAS-warn

The HELAS-ERROR messages appear if the inputs *cannot* be accepted as suitable inputs, such as a negative mass, a tachyonic momentum *etc.* The HELAS-warn messages appear if the inputs *may* have some mistakes, being unusual, but there may not necessarily be errors.

Additionally, we supply a 'scalar polarization' option for the external vector boson subroutine VXXXXX in HELAS_CHECK, so that you can check the program by making use of the BRS invariance of the scattering amplitudes (See the next subsection):

(c) 'scalar polarization' option

We recommend you to link the HELAS_CHECK first and perform a test-run. For the main-run, you should use HELAS which runs much faster than HELAS_CHECK.

4. 2 BRS invariance tests

The use of HELAS_CHECK helps us finding bugs in our program. Also, since all our external particle wavefunctions are fixed unambiguously in terms of their four-momenta and helicities in a given Lorentz frame, Lorentz invariance of the helicity summed squared amplitudes provides us with a good test of the program.[8] However, although these tests will tell us that there are no obvious errors in our program, they won't guarantee that the program actually gives the correct amplitudes. We find that a test of the BRS invariance[9] of scattering amplitudes with one or more external vector bosons can guarantee the correctness of the helicity amplitudes, up to an overall multiplicative constant factor common to all the diagrams of a gauge invariant set. Not only the test provides us with an excellent proof of the correctness of the amplitudes but also will it test the numerical accuracy of the program against the subtle gauge theory cancellations as explained in sect. 3. We have therefore introduce a 'scalar polarization' option to the external vector boson wavefunction subroutine VXXXXX in HELAS_CHECK, so that you can perform the test easily.

There are occasions when the calculation of the amplitudes in the renormalizable R_ξ gauge, the t'Hooft–Feynman gauge in particular, of the electroweak theory can be useful. We find, however, that the use of the covariant R_ξ gauge for the weak boson propagators inside a tree-level helicity amplitude does not lead to a non-trivial test of the amplitude, nor does it lead to a superior numerical accuracy at high energies as compared to the unitary gauge manipulation. We therefore choose all the massive vector boson propagators to take the unitary gauge form in the HELAS subroutines.

What we find most efficient in testing the helicity amplitudes with one or more external vector bosons is the BRS identity,[9]

$$< phys; \mathrm{out} \,|\, (\partial^\mu V_\mu - \xi_V m_V \chi_V) \,|\, phys; \mathrm{in} > = 0 \quad , \tag{7}$$

where ξ_V is the covariant R_ξ gauge parameter and χ_V is the Goldstone mode associated with the vector boson V. The states $< phys; \mathrm{out}\,|$ and $|\,phys; \mathrm{in} >$ are arbitrary physical states of on-shell external particles. By using the reduction formula, the identity (7) leads to an exact relationship between the S-matrix elements of the four-divergence of the vector boson and those of the associated Goldstone boson,

$$< phys, V_S; \mathrm{out} \,|\, phys; \mathrm{in} > = \; - < phys, \chi_V; \mathrm{out} \,|\, phys; \mathrm{in} > \quad , \tag{8}$$

where V_S denotes the 'scalar' component of the vector boson. Eq. (8) relates an amplitude with a V_S emission, which is obtained from the vector boson emission amplitude with the replacement

$$\epsilon_V^\mu(p_V, \lambda_V, S_V) \longrightarrow \frac{p_V^\mu}{m_V} \quad , \tag{9}$$

and the amplitude with an emission of the associated Goldstone boson χ_V. The amplitudes with the Goldstone boson emission are often very simple and can easily

Table 7: The HELAS system.

file name	file size
HELAS.FOR	119 kbytes
HELAS_CHECK.FOR	191 kbytes
HELAS.LIST1	58 kbytes
HELAS.LIST2	4 kbytes
example programs	

be evaluated numerically with HELAS, in some cases even analytically. It is worth noting that the identity (8) between the matrix elements does not depend explicitly on the gauge parameter ξ_V and that it is valid even in the unitary gauge limit $\xi_V \to \infty$. The standard HELAS subroutines can hence be used in the test. The identity turns out to be very efficient in testing the amplitudes as well as the numerical accuracy of the program. See Ref. [1] for more details.

In order to perform the tests conveniently, the vector boson wave function subroutine VXXXXX has an option NHEL = 4 in the checking program HELAS_CHECK.FOR, for which the polarization vector is simply its four-momentum,

$$\epsilon_V^\mu(p_V, \lambda_V = 4) = \epsilon_V^\mu(p_V, \lambda_V = 4)^* = \begin{cases} p_V^\mu / m_V & \text{when } m_V \neq 0 \,, \\ p_V^\mu / p_V^0 & \text{when } m_V = 0 \,. \end{cases} \tag{10}$$

Simply by setting the helicity of an external vector boson to be '4', you can calculate the amplitude for the V_S emission. The HELAS subroutines for the VVS, VSS and VVSS vertices are found to be useful in calculating the associated Goldstone boson emission amplitudes.

§5. How to get HELAS

A complete set of the HELAS files are listed in Table 7. HELAS.FOR and HELAS_CHECK.FOR are packages of FORTRAN77 subroutines. HELAS.LIST1 contains a list, as well as brief descriptions of the inputs and outputs of each HELAS subroutine. When you become accustomed to HELAS, a much shorter list, HELAS.LIST2, will suffice when coding programs.

The subroutine packages HELAS.FOR and HELAS_CHECK.FOR, together with HELAS.LIST1, HELAS.LIST2 and some example programs are available on request from the authors (Bitnet address: murayama@jpnkekvx). The manual of the complete HELAS system has been published as a KEK-Report.[1]

The HELAS system has already been used to study many interesting processes, especially in e^+e^- collision processes since it was developed in collaboration with the members of the JLC (Japan Linear Collider) physics working group. The reported studies include various single vector boson production processes[10]

$$e^+e^- \to e^\pm \overset{(-)}{\nu_e} W^\mp, \; e^+e^-Z, \; \nu_e\bar{\nu}_e Z,$$

detailed studies of the process[11]

$$e^+e^- \to W^+W^- \quad (W^\pm \to f\bar{f}),$$

three weak boson productions[12,13]

$$e^+e^- \to W^+W^-Z,\ ZZZ,$$

and di-lepton di-weak boson production processes[14]

$$e^+e^- \to e^{\pm}\overset{(-)}{\nu_e}W^{\mp}Z,\ e^+e^-W^+W^-,\ e^+e^-ZZ,\ \nu_e\bar{\nu}_eW^+W^-,\ \nu_e\bar{\nu}_eZZ.$$

Also reported are the top quark production via e^+e^- annihilation[15]

$$e^+e^- \to t\bar{t}Z,$$

and via the weak boson fusion processes[16]

$$e^+e^- \to \nu_e\bar{\nu}_et\bar{t},\ e^+e^-t\bar{t},$$

as well as the detailed study near the threshold[17]

$$e^+e^- \to t\bar{t} \quad (t \to bW^+,\ \bar{t} \to \bar{b}W^-).$$

HELAS has also been used in studying Higgs production at e'γ' colliders[18]

$$\gamma e^\pm \to \overset{(-)}{\nu_e} W^\pm H,$$

and also in studying the τ-polarization signals in its multiple π decays[19]

$$e^+e^- \to Z \to \tau^+\tau^- \quad (\tau^\pm \to \overset{(-)}{\nu_\tau} + \pi\text{'s}).$$

There may be many more studies in which our HELAS program will be helpful. We hope that you will also find it useful in your studies.

Acknowledgments

The authors would like to thank B.K. Bullock, H. Iwasaki, J. Kanzaki, A. Miyamoto, D. Zeppenfeld, and the members of the JLC (Japan Linear Collider) physics working group for collaborations that contributed to the present form of HELAS.

References

[1] H. Murayama, I. Watanabe and K. Hagiwara, *"HELAS: HELicity Amplitude Subroutines for Feynman diagram evaluations"*, KEK-Report 91-11, Dec. 1991.

[2] T. Kaneko and H. Tanaka, in *"Proceedings of the Second Workshop on Japan Linear Collider (JLC)"*, KEK-Proceedings 91-10, Nov. 1991.

[3] E.E. Boos *et. al.*, Moscow State Univ. Inst. for Nucl. Phys. preprint MGU-89-63/140, Moscow, 1989; DESY preprint, DESY 91-114, Oct. 1991.

[4] S.G. Gorishny, S.A. Larin, L.R. Surguladze and F.V. Tkachov, *Comput. Phys. Commun.* **55** (1989) 381.

[5] J. Küblbeck, M. Böhm and A. Denner, *Comput. Phys. Commun.* **60** (1990) 165: R. Mertig, M. Böhm and A. Denner, *ibid.* **64** (1991) 345.

[6] S. Kawabata, in *"Proceedings of the Second Workshop on Japan Linear Collider (JLC)"*, KEK-Proceedings 91-10, Nov. 1991; *Comput. Phys. Commun.* **41** (1986) 127.

[7] G.P. Lepage, Cornel Univ. preprint CLNS-80/447, Mar 1980.

[8] K. Hagiwara and D. Zeppenfeld, *Nucl. Phys.* **B274** (1986) 1; *ibid.*, **B313** (1989) 560.

[9] C. Becchi, A. Rouet and R. Stora, *Ann. Phys.* **98** (1976) 287.

[10] K. Hagiwara, H. Iwasaki, A. Miyamoto, H. Murayama and D. Zeppenfeld, *Nucl. Phys.* **B365** (1991) 544.

[11] A. Miyamoto, in *"Proceedings of the Second Workshop on Japan Linear Collider (JLC)"*, KEK-Proceedings 91-10, Nov. 1991.

[12] H. Murayama, Doctral Thesis, Univ. of Tokyo preprint, UT-580 (1991).

[13] I. Watanabe, in *"Proceedings of the Second Workshop on Japan Linear Collider (JLC)"*, KEK-Proceedings 91-10, Nov. 1991.

[14] K. Hagiwara, J. Kanzaki and H. Murayama, KEK preprint, KEK-TH-282 (1991).

[15] K. Hagiwara, H. Murayama and I. Watanabe, *Nucl. Phys.* **B367** (1991) 257.

[16] T. Tsukamoto, in *"Proceedings of the Second Workshop on Japan Linear Collider (JLC)"*, KEK-Proceedings 91-10, Nov. 1991.

[17] K. Fujii, in *"Proceedings of the Second Workshop on Japan Linear Collider (JLC)"*, KEK-Proceedings 91-10, Nov. 1991:
Y. Sumino, K. Fujii, K. Hagiwara, H. Murayama and C.-K. Ng, KEK preprint, KEK-TH-284 (1992).

[18] K. Hagiwara, I. Watanabe and P.M. Zerwas, *Phys. Lett.* **B278** (1992) 186.

[19] B.K. Bullock, K. Hagiwara and A.D. Martin, KEK preprint, KEK-TH-332 (1992).